SPECIAL PROJECT FINAL REPORT

All the following mandatory information needs to be provided.

Project Title:	Go Beyond Current Limitations of Climate Simulation and Projection over Land
Computer Project Account:	spitales
Start Year - End Year :	2016 - 2018
Principal Investigator(s)	Andrea Alessandri
Affiliation/Address:	ENEA Bldg C59, CR Casaccia, Via Anguillarese, 301 00123 Santa Maria di Galeria - Rome, Italy
Other Researchers (Name/Affiliation):	Franco Catalano (ENEA), Matteo De Felice (ENEA), Irene Cionni (ENEA), Alessandro Dell'Aquila (ENEA)

The following should cover the entire project duration.

Summary of project objectives

(10 lines max)

The objectives of this special projects are (i) develop a process-based albedo parameterization in EC-Earth, (ii) validate and assess the effects of the new albedo scheme on the simulated climate during the last Century historical period and (iii) evaluate the interactions and feedbacks of the interactive albedo in the future climate projections (CMIP6).
The couplings and feedbacks of the newly introduced interactive albedo will be assessed together with the interactions with the changes of water availability (soil moisture and snow) as well as changes in land cover/land use types.

Summary of problems encountered

(If you encountered any problems of a more technical nature, please describe them here.)

The development and tuning of version 3.3.1 of EC-Earth to be used for CMIP6-LS3MIP projection experiments has been delayed by almost two years and just been released in the frame of the EC-Earth Consortium. Therefore, it was not possible to perform the projection experiments (GLACE-A and GLACE-B) during the timespan of the SPITALES project. However, now that EC-Earth3.3.1 is ready, we plan to perform the climate-projection simulations following the LS3MIP protocol (GLACE A and GLACE B) by the end of the summer and to start beginning of July 2019. To this aim we plan to use HPC resources from member state accounts at ECMWF and/or other HPC infrastructures available at ENEA if necessary (CRESC-04 HPC).

Experience with the Special Project framework

(Please let us know about your experience with administrative aspects like the application procedure, progress reporting etc.)

No problems encountered and we got all information and help needed.

Summary of results

(This section should comprise up to 10 pages, reflecting the complexity and duration of the project, and can be replaced by a short summary plus an existing scientific report on the project.)

1. Improve land surface-vegetation representation in EC-Earth

Novel observational global datasets of land-surface variables are expected to significantly enhance understanding and representation of land surface processes in Earth System Models (ESMs). To this aim latest available albedo (GLCF-GLASS and COPERNICUS), Leaf Area Index (GLCF-GLASS and COPERNICUS), snow extent (NSIDC), soil moisture (ESA) and ECMWF reanalysis for surface temperature and precipiation (ERA-INTERIM/ERA5) have been analyzed to identify the most relevant processes that contribute to vegetation-climate interactions and feedbacks. The analysis unveiled novel important observational constraints (Alessandri et al., 2019) that have driven the development of new process-based parameterizations in HTESSEL (i.e. the land-surface model included in the EC-Earth ESM; Hurk et al., 2003; Balsamo et al., 2009).
The observationally-based formulation of extinction of light below the vegetation canopy has been exploited to derive an interactive computation of the effective cover of vegetation over bare ground (included in EC-Earth starting from version 2.4; Alessandri et al. 2017). The improved representation of vegetation processes has been included in the latest available version of EC-Earth (v3.3.1.1). The year-to-year variations in land use cover has been implemented in collaboration with

the colleagues at Lund University and prescribed from the LUH2 dataset (http://luh.umd.edu/; Hurtt et al. 2011).

1.1. Develop a process-based albedo parameterization in EC-Earth

HTESSEL subgrid discretization:
HTESSEL (Balsamo et al. 2009) discretization, for each grid point, solves for up to six different land surface tiles that may be present over land (bare ground, low and high vegetation, intercepted water by vegetation, and shaded and exposed snow). Surface radiative, latent heat and sensible heat fluxes are calculated as a weighted average of the values over each tile. The background tile fractions (bare ground, A_b, low and high vegetation maximum fractional coverages, $A_{l,h}$) are prescribed from a static land-use map (or provided by LPJ-Guess, Smith et al., 2014, when vegetation dynamics turned on) ensuring that each grid point sum to unity:

$1 = A_l \times C_l + A_h \times C_h + A_b$ (1)

In (1), $C_{l,h}$ is the density of vegetation that is parameterized according to the Lambert Beer (LB) law of extinction of light under a vegetation canopy (included in EC-Earth starting from version 2.4, while tabled values were used before; Alessandri et al., 2017):

$C_{l,h} = 1 - exp(-0.5LAI_{l,h})$ (2)

And so the actual vegetation cover (hereinafter effective vegetation cover, Ceff):

$Ceff_{l,h} = A_{l,h}\,[1 - exp(-0.5LAI_{l,h})]$ (3)

A new process-based parameterization of albedo over snow-free areas has been developed in HTESSEL. Given the HTESSEL discretization, it follows that total albedo (A_{tot}) in each grid-point [i, j] can be represented as the weighted average of the vegetation ($A_{lveg,hveg}$) and of the bare soil (A_{soil}) components:

$$\begin{aligned} A_{tot}(i,j,t) = & \\ & = A_{lveg}[lveg = TVL, i, j, t] * C_{eff,l}(i,j,t) \\ & + A_{hveg}[hveg = TVH, i, j, t] * C_{eff,h}(i,j,t) \\ & + A_{soil}(i,j,t) * [1 - C_{eff,l}(i,j,t) - C_{eff,h}(i,j,t)] \end{aligned}$$

where TVL (TVH) is the dominant low (high) vegetation type and $C_{eff,l,h}$ is the effective cover for low (l) and high (h) vegetation, respectively. Vegetation albedo is obtained from lookup-table values that are estimated, from available observations, for each of the 10 low-vegetation PFTs (A_{lveg}; lveg=1,…,10) and 6 high-vegetation PFTs (A_{hveg}; hveg=1,…,6) considered in HTESSEL. See Section 1.2 for the details on the different methodologies employed to estimate Vegetation look-up table and soil albedo.

1.2. Methodologies employed to estimate Vegetation look-up table and soil albedo

Several methods have been tested and compared in order to parameterize the interactive behaviour of vegetation and soil albedo. To be able to describe/compare all methods using the same notation, we use the general formalism that can be associated to any estimation based on minimization of Norms $||\ ||_p$ (p=1,2,3,....; also often indicated as L^p-Norms):

$$||x||_p = \sum_i (x_i{}^p)^{1/p}$$

All methods have been applied/compared on the native reduced gaussian grid used in IFS (standard resolution) and using area weighting according to the relative grid-point areas. The snow-free monthly MODIS albedos and LAI data are used in the same reduced gaussian grid as defined in the boundary conditions file for IFS (ICMCL file; Morcrette et al., 2008). On the other hand the independent GLCF albedo data (Liu et al., 2013) had to be interpolated from regular 0.05°x0.05° longitude/latitude grid into the same reduced Gaussian grid for comparison. Similarly, the LAI3g

leaf area index (LAI; Zhu et al., 2013) data have been interpolated from original 0.5°x0.5° regular grid.

REGRESSION METHOD (REG)

Assumptions:

-HTESSEL subgrid discretization is assumed as representative of real world.

-Albedo soil map from Rechid et al. (2009) is assumed as perfect.

L^2-Norm is used in the following regression:

$$min \left\| \frac{A_{Reg,\,lveg,\,hveg} - Atot_{obs}\left(1 - Ceff_{L,H}\right) * Asoil_{Rechid}}{Ceff_{L,H}} \right\|_2$$

ESTIMATE METHOD [EST]

Assumptions:

-HTESSEL subgrid discretization is assumed as representative of real world.

-A threshold for the effective vegetation cover ($Ceff_{l,h}$) is assumed as filter for the selection of grid points representative of each specific vegetation type.

Priority is given to the estimation of the vegetation look-up table parameters. Approach is conservative to avoid overfitting of the data and related error compensation.

In the following the minimization problem that has been used:

$$min \left\| A_{ext,\,lveg,\,hveg} - Atot_{obs} \right\|_2$$

only for $Ceff_{l,h}$ > max_threshold_lveg,hveg and lveg=TVL or hveg=TVH

where max_threshold_lveg,hveg for $Ceff_{L,H}$ is the result of an iterative selection procedure, for each vegetation type, that tries to get by one hand the maximum threshold possible while, on the other hand, ensuring a large and robust sample for the estimate (convergence of estimates and Gaussian behaviour of the sample frequency distribution). Note that Ceff is the effective (meaning actual) vegetation cover and not $A_{l,h}$ i.e. the max theoretical vegetation cover (meaning the area not occupied by other type of cover, i.e. lakes, land ice). The threshold is chosen [arbitrarily] with the objective to obtain large enough sample of data so that the samples are as much as possible representative of a population with random and independent sampling errors in the estimates.

Solution of this minimization problem is simply the average of the sample for each vegetation type. Associated to each vegetation-type estimate, we can obtain the uncertainty bounds using the percentiles in the corresponding normal distribution of the sample.

ESTIMATE + ESTIMATE-new-MAP METHOD [EST+newmap]

Same as ESTIMATE method but assuming that the vegetation albedo look-up table provided by ESTIMATE is perfect estimate.

The above assumption allows to solve for an additional minimization problem for a soil albedo map $A_{soil,ext}$ that is consistent with the look-up table values computed using ESTIMATE:

$$min\,||\,Atot_{obs}(i,j,t) - Aveg_{ext,\,lveg=TVL(i,j)} * Ceff_L(i,j,t) - Aveg_{ext,\,hveg=TVH(i,j)} * Ceff_H(i,j,t) -$$

$$- A_{soil,ext}(i,j)\left[1 - Ceff_L(i,j,t) - Ceff_H(i,j,t)\right]||_1$$

The soil albedo maps (hereinafter ESTIMATE-new-MAP) have been estimated for the two spectral bands and the two components (parallel and diffuse). Minimum and maximum acceptable values of observable soil albedos were obtained from available atlases from geographers/pedologists (e.g. Dickinson et al., 1993, Hartmann et al. 1994). For each grid point we checked that the obtained soil albedo values stay within the observable range and corrected the values accordingly when necessary.

Soil Look-up Table Method [SLT]

A soil look-up table is estimated following a similar method than for the look-up table of vegetation (ESTIMATE). The objective is to estimate a specific albedo of soil ($Asoil_{isoil}$) to each of seven soil categories defined in HTESSEL based on different textures: Coarse, Medium, Medium-fine, Fine, very fine, organic, tropical organic.

Assumptions:

-HTESSEL subgrid discretization is assumed as representative of real world.

-A max threshold for the effective vegetation cover ($Ceff_{tot}$) is assumed as filter for the selection of grid points representative of each specific soil types.

-Deserts are excluded by selecting only those points where vegetation is theoretically possible and so where structured soil is in place (in contrast with deserts where soils are not present), that is where $A_{l,h}$ (i.e. the max theoretical vegetation cover) is large enough, i.e. CVL+CVH>0.5.

The soil albedo look-up table values have been estimated for the two spectral bands and the two components (parallel and diffuse) by selecting the grid points where the total effective vegetation cover is small enough, and such that the measures can be attributed to points dominated by one of possible soil types (soil_type=isoil; no coexistence of more than one soil-type is possible in HTESSEL):

(CVeff_tot)<threshold_soil

where CVeff_tot is the total effective vegetation cover for high and for low vegetation

$min \left\| A_{slt,isoil} - Atot_{obs} \right\|_2$ only for $Ceff_l + Ceff_h <$ min_threshold and for each soil_type=isoil

1.2.1. Experiments and comparison of the different methodologies

The performance of the different albedo parameterizations has been analyzed on a set of historical simulations with AMIP-type (using HadISST SST and sea ice [Rayner et al. 2003] from the CMIP6 forcing dataset input4MIPs) setup spanning 28 years (1982-2009) with the development-version 3.2 of EC-Earth (see Table 1 for a summary of experiments performed). Three members have been performed for each experiment. In all simulations, the vegetation LAI variability is prescribed from the LAI3g dataset based on the third generation GIMMS and MODIS satellite observations (Zhu et al., 2013). The model version used for all the experiments also include the enhanced vegetation sensitivity described in Alessandri et al. (2017). In the MODIS experiments the albedo is prescribed from satellite-derived MODIS monthly climatology (Morcrette et al. 2008) as in the current version of IFS/HTESSEL.

Experiment name	Albedo parameterization
MODIS	Climatological snow-free albedo from MODIS
EST+SLT	Vegetation albedo from EST, soil albedo from SLT
REG+Rechid	Vegetation albedo from REG, soil albedo from Rechid map

EST+newmap	Vegetation albedo from EST, new soil albedo map

Table 1. Summary of AMIP experiments performed with EC-Earth v3.2. Period: 1982-2009, three members, LAI prescribed from LAI3g observations.

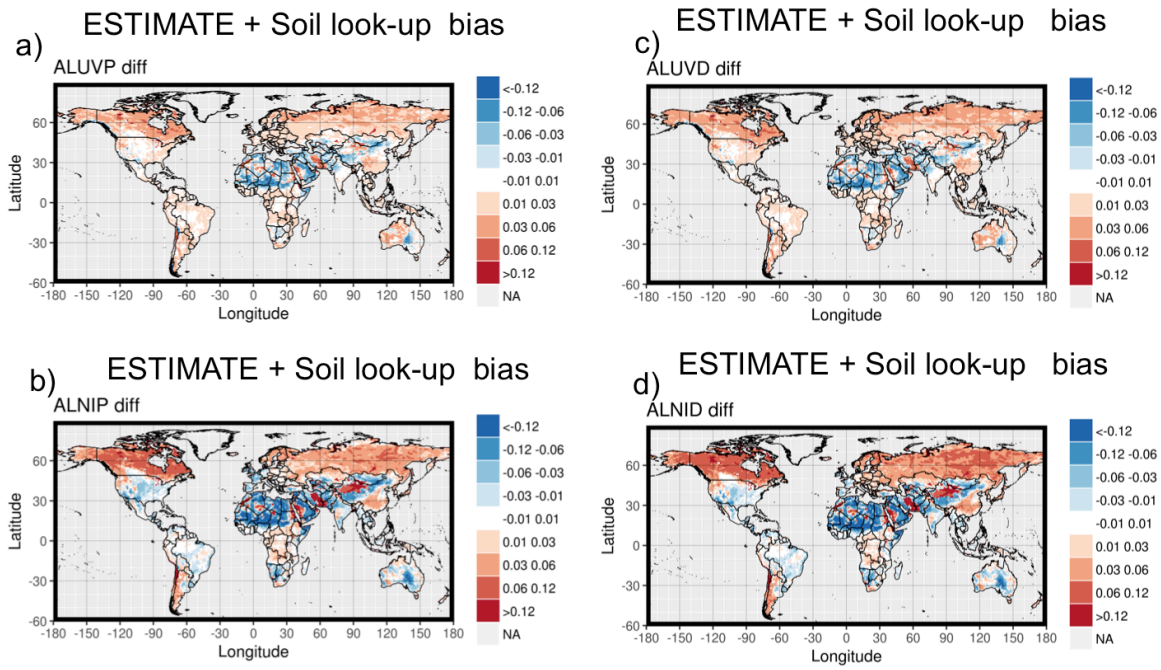

Figure 1: ESTIMATE+Soil look-up table bias: Annual average of difference between simulated and MODIS albedo in the different spectral bands in the ESTIMATE+Soil look-up table case (ALUVP=visible, direct; ALUVD=visible, diffuse; ALNIP=near infrared, direct; ALNID=near infrared, diffuse).

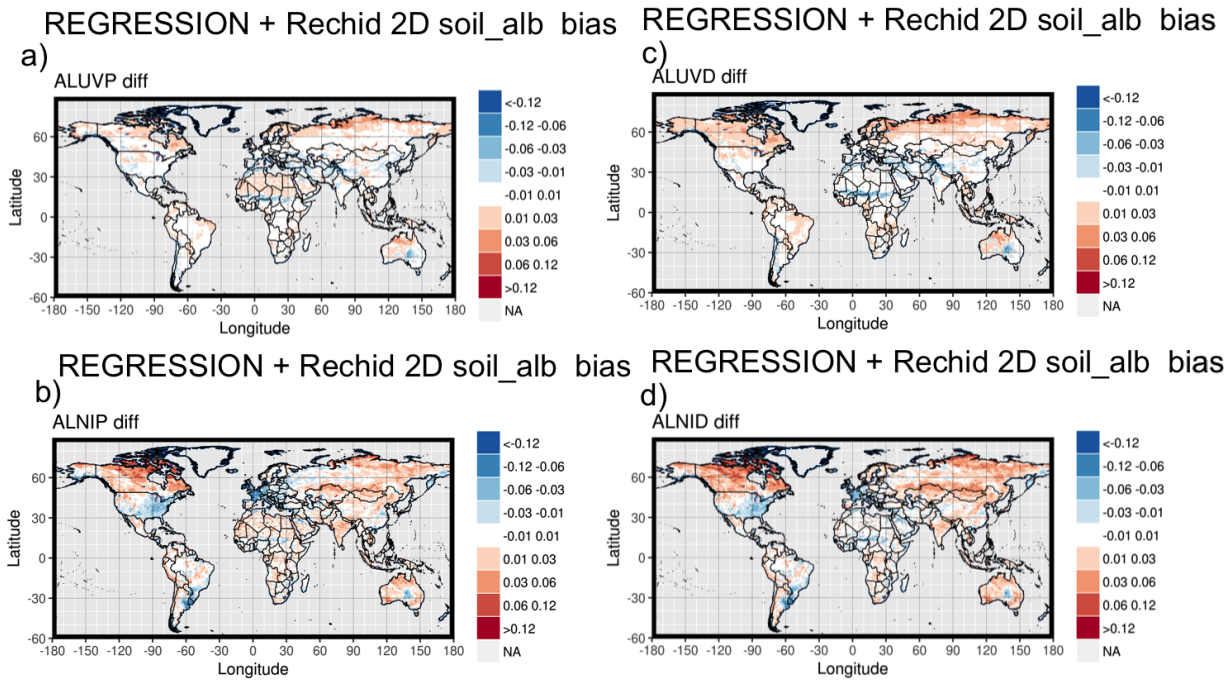

Figure 2: Same as Figure 1 but for REGRESSION + Rechid 2D soil albedo map. Fixed soil albedo map from Rechid et al. (2009).

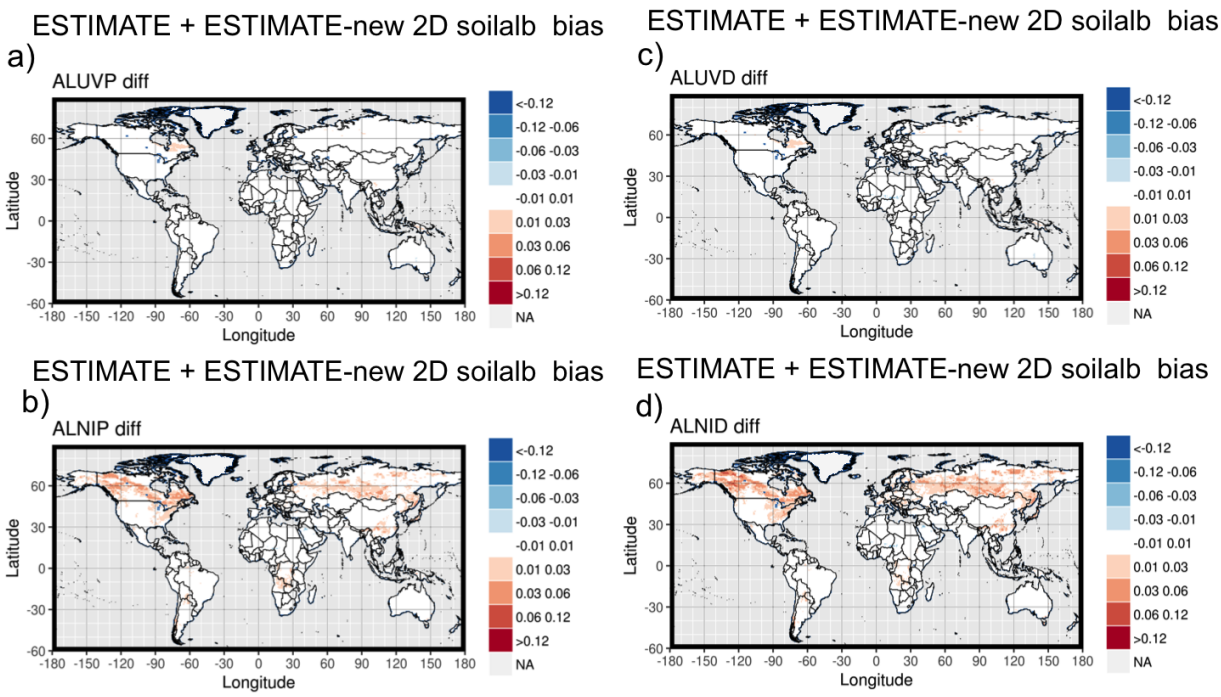

Figure 3: Same as Figure 1 but for ESTIMATE + ESTIMATE-new 2D soil albedo map

BIAS (RMSE)	ANN	JJA	DJF
ESTIMATE + Soil look-up table	0.05 (0.31)	0.01 (0.27)	0.05 (0.44)
REGRESSION + Rechid 2D soil_alb	-0.02 (0.16)	0.03 (0.44)	-0.03 (0.37)
ESTIMATE + ESTIMATE-new 2D soil_alb	0.00 (0.15)	0.01 (0.27)	0.01 (0.29)

Table 2. Global mean bias (and RMSE in brackets) of 2m-temperature with respect to control simulation with prescribed MODIS

Compared to REG+Rechid and EST+newmap, that use 2D gridded estimates of the background soil albedo, the method employing the soil look-up table (Figure 1) introduces a discretization of the representation in soil classes that reduces the performance in reproducing the MODIS albedo. The associated 2m-temperature biases and RMSE tend to be compensated on a global average. The use of a fixed soil albedo map produces significantly better results, except for June-July-August (JJA).

1.3. Implementation of the soil albedo dependence on soil moisture

The albedo over bare soil is represented by a novel parameterization, which accounts for the dependence upon soil moisture (SM). The relation between albedo and SM has been estimated by using the latest global observational datasets of parallel and diffuse albedo (visible and near-infrared bands) from COPERNICUS global land service (https://land.copernicus.eu/global/) and SM from the latest ESA product (Dorigo et al. 2017). To obtain snow-free albedo from the COPERNICUS data, we used the snow extent dataset from NOAA (Brown and Robinson 2011) to

filter out for each time all land points where snow is present. More than 50% of the grid-points of the global albedo land-domain (space-time) is marked as snow-free and used in the analysis.
We distinguish soil albedo (A_{soil}) into two components: (i) constant background map from Rechid et al (2009; $A_{soil,Rechid}$) and (ii) time varying soil albedo anomalies ($A_{soil,anom}$), where $A_{soil,Rechid}$ represents time-invariant soil albedo inhomogeneities in space [i, j], while $Alb_{soil,anom}$ are dependent on soil moisture variability in time [t]:

$$A_{soil}(i,j,t) = A_{soil,Rechid}(i,j) + A_{soil,anom}(SM[i,j,t], texture[i,j], color[i,j])$$

The link between $A_{soil,anom}$ and SM depends on two properties in the soil: (i) texture and (ii) color. Soil color map from Wilson and Henderson-Sellers (1985; Figure 4, right) considers 9 soil colors, from light (1) to dark (8) and one additional class (9) for deserts. HTESSEL soil texture map, derived from the FAO/UNESCO Digital Soil Map of the World (FAO, 2003), distinguishes 7 soil types (Figure 4, left): coarse, medium, medium-fine, fine, very-fine, organic, tropical-organic. By combining colour and texture information of the soil, we divided the land areas into 9*7=63 soil classes. For each soil class, bare soil albedo information has been obtained using COPERNICUS total albedo dataset for each of the four short-wave bands represented in the IFS radiation code (visible and near infrared for both diffuse and parallel beams) by removing albedo of vegetation fraction (Rechid et al. 2009, Otto et al. 2011). Furthermore, grid-points with very high vegetation cover (>0.8) have been excluded.
In-situ measurements revealed both exponential (Liu et al. 2014, Guan et al. 2009) and linear (Li et al. 2019) relations between soil albedo and soil moisture, depending on the soil characteristics. Accordingly, for each soil class we seek robust (statistically significant) exponential or linear relations between soil albedo anomalies and soil moisture for the four short-wave bands. Exponential regression functions and their significance is estimated by using the algorithm developed by Bates and Chambers (1992) in its R implementation. Where exponential regression does not converge or is not significant a linear regression is sought. An R implementation of the F-test (Chambers 1992) is used to test significance of linear regressions. As an example, Figure 5 shows the scatterplots between the near-infrared parallel component of $A_{soil,anom}$ versus SM for two texture/color classes, together with the regression functions as identified by our method and that passed statistical significance (10% significance level) for each case.
Figure 6 shows the scatterplots between the near-infrared parallel component of $A_{soil,anom}$ versus SM for the different colour/texture combinations, together with the regression functions that passed statistical significance for each case. It is clear from the figure how the regression functions for the different texture/color classes captures the variability of soil albedo anomalies that is related with SM. Scatterplots for the visible components show similar results but with different albedo ranges (not shown).

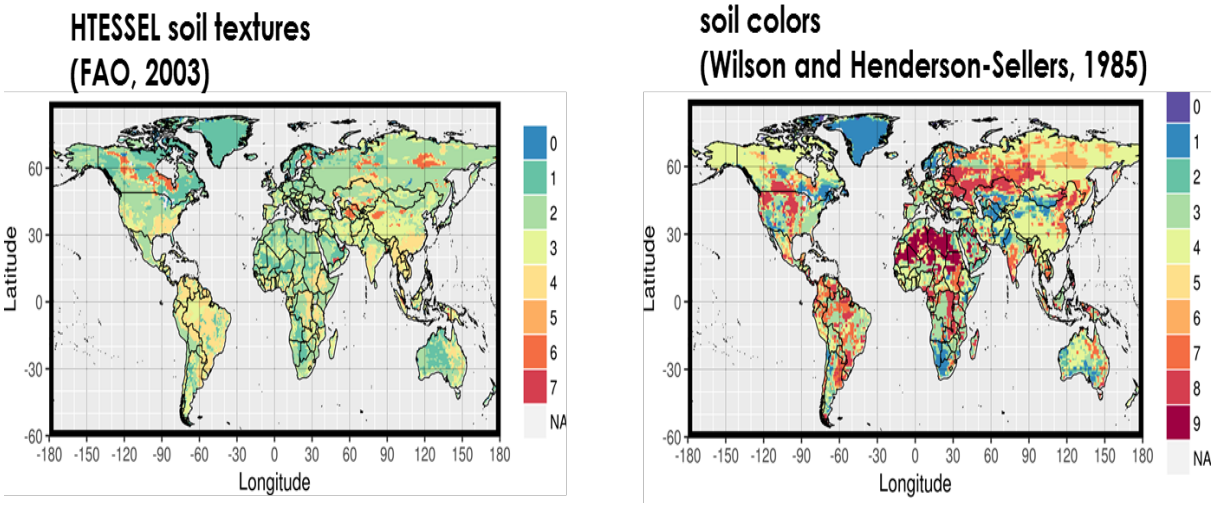

Figure 4: Soil texture (left panel) and soil color (right panel) classes.

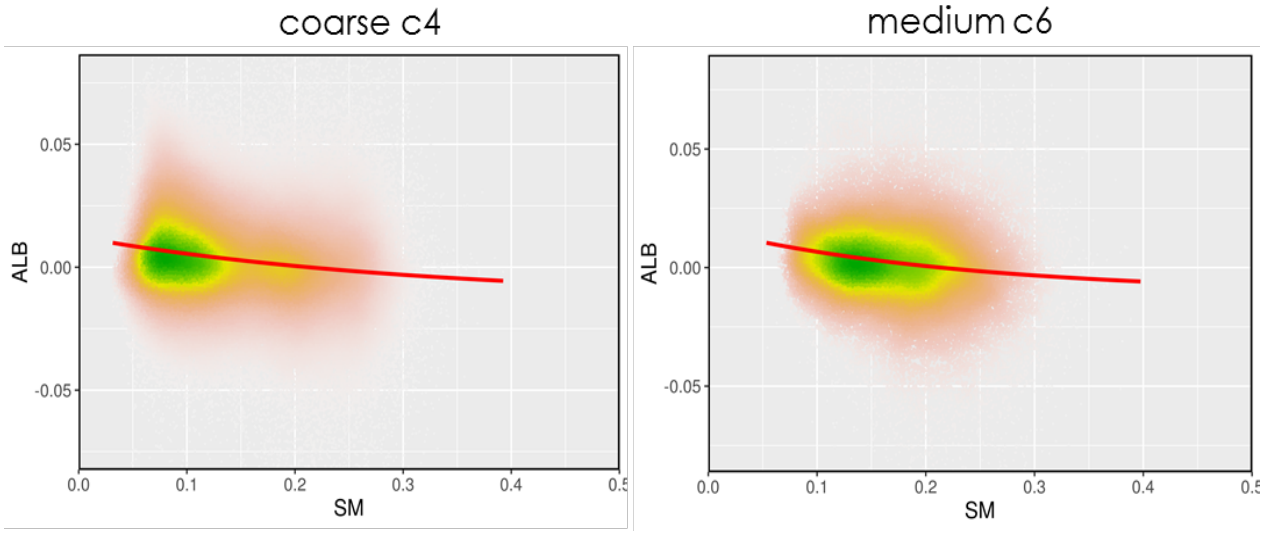

Figure 5: Scatterplot the of the near-infrared component of Asoil anomalies vs Soil Moisture for coarse c4 and medium c6 classes. Red lines are the significant (1% significance level) regression curves for each texture/color class. Point colors indicate scatter density (from light brown (lower) to green (higher))

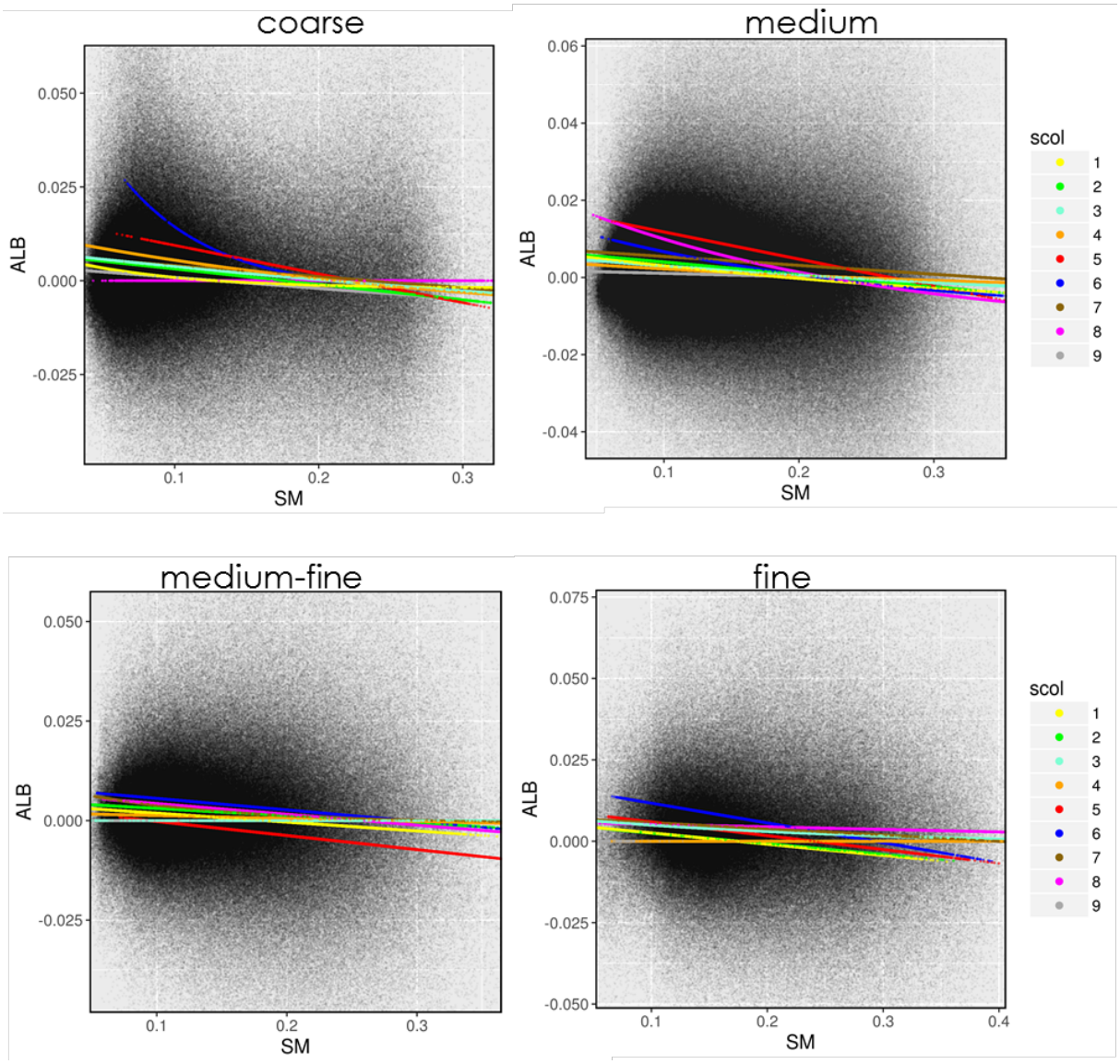

Figure 6: Scatterplot the of the near-infrared component of Asoil anomalies vs Soil Moisture for the more represented 4 texture classes. Color lines are the significant (1% significance level) regression curves for each texture/color class.

1.3.1. Sensitivity to the new soil albedo scheme with dependence on soil moisture

A set of historical simulations covering the last century (1900-2014) have been performed using version 3.2.3 of EC-Earth (with bug-fix from development branch: r5872-LundUniDevBranch) in order to evaluate the sensitivity to the new soil albedo scheme with dependence on soil moisture. In particular, to validate the albedo simulated by the new scheme against available satellite observations, two AMIP-type simulations have been performed over the period 1982-2015. The experiment that includes the new process-based soil albedo parameterization (SENS) is compared with control simulation that uses constant soil albedo map from Rechid et al., (2009; CTRL) and for both CTRL and SENS vegetation LAI has been prescribed from the observational LAI3g dataset (Zhu et al. 2013).

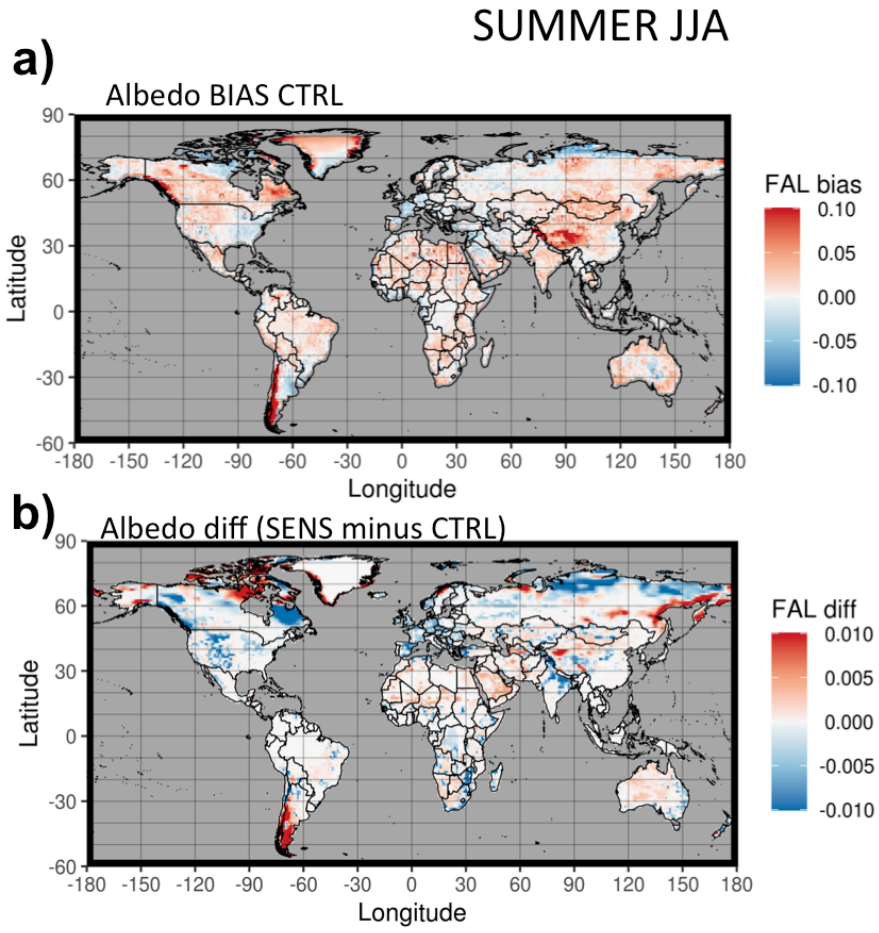

Figure 7: Boreal Summer (June–July–August) a) surface albedo bias of CTRL with respect to GLCF observational data and b) sensitivity (SENS minus CTRL difference).

The analysis of the AMIP-type simulation shows that CTRL has a positive surface albedo bias in most regions when compared with GLCF satellite data (Figure 7a). The experiment that includes the new process-based soil albedo parameterization improves by reducing the bias in several regions (Figure 4b). In particular, the bias is considerably reduced over high-latitude North America and Asia as well as Europe and Central US. On the other hand, a slight increase of the positive bias is found over Sahara and Arabian deserts. Accordingly, the surface albedo simulated in SENS tends to display higher anomaly correlation with GLCF broadband albedo from satellite (Figure 8). The SENS minus CTRL correlation difference shows some improvements over middle to high latitudes. The only exception is high latitude Siberia and North-East Canada. In this respect, it is noted that these high latitude regions can be partially covered by snow during boreal summer and therefore the difference in the anomaly correlation could be as well explained by random effects related to the internal variability of snow cover extent that cannot be avoided in the AMIP-type set-up of the experiments. Also, the internal variability in the soil moisture doesn't ensure that soil moisture

anomalies are realistically simulated in the AMIP-type experiments, therefore affecting the evaluation of the beneficial effects of the new soil albedo scheme. More analysis and experimentation will be needed to obtain robust estimates of the effects of the new soil albedo scheme.

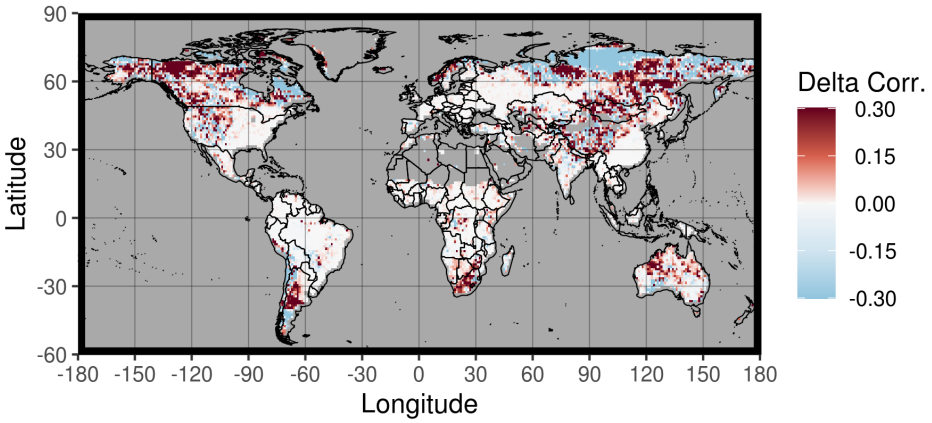

Figure 8: SENS minus CTRL *Boreal Summer (June–July–August) surface albedo anomaly correlation difference. Reference observation is GLCF satellite data.*

1.4. CMIP6-LS3MIP setup and delayed climate-projection simulations

In collaboration with colleagues from Lund University we have finalised the technical interface to prescribe land-surface states in HTESSEL-IFS for the experiments following the LS3MIP protocol (Hurk et al., 2016), which requires to prescribe land surface states at daily frequency. It is required reading external files daily and replacing land surface variables throughout the entire simulations. A nudging procedure for soil moisture content has been developed and implemented in a dedicated 'ls3mip' branch in the development portal of the EC-Earth ESM model.
Although the technical interface to prescribe land-surface states for the projection experiments following the LS3MIP protocol was implemented in due time, it was not possible to perform the projection experiments (GLACE-A and GLACE-B) as planned in the SPITALES project. The reason is that the development and tuning of EC-Earth3.3.1 (to be used for CMIP6-LS3MIP) has been delayed by several months and just been released in the frame of the EC-Earth Consortium. Accordingly we plan to perform the climate-projection simulations following the LS3MIP protocol (GLACE A and GLACE B) by the end of the summer and to start beginning of July 2019. To this aim we plan to use HPC resources from member state accounts at ECMWF and/or other HPC infrastructures available at ENEA if necessary (CRESC-04 HPC).

References

Alessandri A., Catalano F., De Felice M., van den Hurk B., Doblas-Reyes F., Boussetta S., Balsamo G., Miller P. A., 2017: Multi-scale enhancement of climate prediction over land by increasing the model sensitivity to vegetation variability in EC-Earth. Clim. Dyn., 49, 1215-1237, doi:10.1007/s00382-016-3372-4

Balsamo, G., A. Beljaars, K. Scipal, P. Viterbo, B. van den Hurk, M. Hirschi, and A. K. Betts, 2009: A revised hydrology for the ECMWF model: Verification from field site to terrestrial water storage and impact in the integrated forecast system. J. Hydrometeor. , 10 , 623–643, doi:10.1175/2008JHM1068.1.

Bates, D. M. and Chambers, J. M. (1992) Nonlinear models. Chapter 10 of Statistical Models in S eds J. M. Chambers and T. J. Hastie, Wadsworth & Brooks/Cole.

Brown, R. D. and Robinson, D. A.: Northern Hemisphere spring snow cover variability and change over 1922–2010 including an assessment of uncertainty, The Cryosphere, 5, 219-229, https://doi.org/10.5194/tc-5-219-2011, 2011

Chambers, J. M. (1992) Linear models. Chapter 4 of Statistical Models in S eds J. M. Chambers and T. J. Hastie, Wadsworth & Brooks/Cole.

Dickinson, R. E., A. Henderson-Sellers, and P. J. Kennedy, 1993: *Biosphere-atmosphere Transfer Scheme (BATS) Version 1e as Coupled to the NCAR Community Climate Model*. NCAR Technical Note NCAR/TN-387+STR, doi:10.5065/D67W6959

Dorigo, W., et al., 2017: ESA CCI Soil Moisture for improved Earth system understanding: State-of-the art and future directions, Remote Sensing of Environment, 203, 185-215, doi:10.1016/j.rse.2017.07.001

FAO (2003). Digital soil map of the world (DSMW). Technical report, Food and Agriculture Organization of the United Nations, re-issued version.

Guan, X., Huang, J., Guo, N., Bi, J., Wang, G., 2009: Variability of soil moisture and its relationship with surface albedo and soil thermal parameters over the Loess Plateau. Advances in Atmospheric Sciences, 26 (4), pp. 692-700, DOI: 10.1007/s00376-009-8198-0

Hartman, D.L., 1994: Global Physical Climatology , Internationa Geophysics Series, Ed. R. Dmowska and J.R. Holton, Academic Press, Vol. 56, 411 pp.

Hurk van den, BJJM., Viterbo P, Los SO (2003) Impact of leaf area index seasonality on the annual land surface evaporation in a global circulation model. J Geophys Res 108(D6):4191. doi:10 .1029/2002jd002846

Hurk van den, BJJM., Kim, H., Krinner, G., Seneviratne, S. I., Derksen, C., Oki, T., Douville, H., Colin, J., Ducharne, A., Cheruy, F., Viovy, N., Puma, M. J., Wada, Y., Li, W., Jia, B., Alessandri, A., Lawrence, D. M., Weedon, G. P., Ellis, R., Hagemann, S., Mao, J., Flanner, M. G., Zampieri, M., Materia, S., Law, R. M., and Sheffield, J., 2016: LS3MIP (v1.0) contribution to CMIP6: the Land Surface, Snow and Soil moisture Model Intercomparison Project – aims, setup and expected outcome, Geosci. Model Dev., 9, 2809-2832, doi:10.5194/gmd-9-2809-2016.

Li, Z., Yang, J., Gao, X., Yu Y., Zheng Z., Liu R., Wang C., Hou X., Wei Z., 2019: The relationship between surface spectral albedo and soil moisture in an arid Gobi area. Theor Appl Climatol (2019) 136: 1475. https://doi.org/10.1007/s00704-018-2577-3

Liu, S., Roujean, J.-L., Kaptue Tchuente, A.T., Ceamanos, X., Calvet, J.-C., 2014: A parameterization of SEVIRI and MODIS daily surface albedo with soil moisture: Calibration and validation over southwestern France. Remote Sensing of Environment, 144, pp. 137-151, DOI: 10.1016/j.rse.2014.01.016

Liu, Q., L. Wang, Y. Qu, N. Liu, S. Liu, H. Tang, and S. Liang, 2013: Preliminary evaluation of the long-term glass albedo product. International Journal of Digital Earth, 6 (sup1), 69–95, doi:10.1080/17538947.2013.804601, https://doi.org/10.1080/17538947.2013.804601

Morcrette, J.-J., Barker, H. W., Cole, J. N. S., Iacono, M. J., Pincus, R.,, 2008: Impact of a New Radiation Package, McRad, in the ECMWF Integrated Forecasting System. Mon. Wea. Rev., 136, 4773-4798.

Otto, J., T. Raddatz, and M. Claussen, 2011: Strength of forest-albedo feedback in mid-Holocene climate simulations, Clim. Past, 7, 1027-1039, doi:10.5194/cp-7-1027-2011

Rayner, N. A.; Parker, D. E.; Horton, E. B.; Folland, C. K.; Alexander, L. V.; Rowell, D. P.; Kent, E. C.; Kaplan, A. (2003) Global analyses of sea surface temperature, sea ice, and night marine air temperature since the late nineteenth century J. Geophys. Res.Vol. 108, No. D14, 4407 10.1029/2002JD002670

Rechid, D., T. J. Raddatz, and D. Jacob, 2009: Parameterization of snow-free land surface albedo as a function of vegetation phenology based on MODIS data and applied in climate modelling, Theor. Appl. Climatol., 95, 245-255, doi:10.1007/s00704-008-0003-y

Wilson, M. F. and Henderson□Sellers, A. (1985), A global archive of land cover and soils data for use in general circulation climate models. J. Climatol., 5: 119-143. doi:10.1002/joc.3370050202

Zhu, Z., Bi, J., Pan, Y., Ganguly, S., Anav, A., Xu, L., Samanta, A., Piao, S., Nemani, R. R., and Myneni, R. B., 2013: Global Data Sets of Vegetation Leaf Area Index (LAI)3g and Fraction of Photosynthetically Active Radiation (FPAR)3g Derived from Global Inventory Modeling and Mapping Studies (GIMMS) Normalized Difference Vegetation Index (NDVI3g) for the Period 1981 to 2011, Remote Sens., 5, 927–948.

List of publications/reports from the project with complete references

- Alessandri, F. Catalano, M. De Felice, B. Van Den Hurk, F. Doblas Reyes, S. Boussetta, G. Balsamo, and P. Miller, 2016: Multi-scale enhancement of climate prediction over land by increasing the model sensitivity to vegetation variability in EC-Earth, Clim. Dyn, 49: 1215. doi:10.1007/s00382-016-3372-4, link to-readcube document http://rdcu.be/kJuG
- van den Hurk, B., Kim, H., Krinner, G., Seneviratne, S. I., Derksen, C., Oki, T., Douville, H., Colin, J., Ducharne, A., Cheruy, F., Viovy, N., Puma, M. J., Wada, Y., Li, W., Jia, B., Alessandri, A., Lawrence, D. M., Weedon, G. P., Ellis, R., Hagemann, S., Mao, J., Flanner, M. G., Zampieri, M., Materia, S., Law, R. M., and Sheffield, J., 2016: LS3MIP (v1.0) contribution to CMIP6: the Land Surface, Snow and Soil moisture Model Intercomparison Project – aims, setup and expected outcome, Geosci. Model Dev., 9, 2809-2832, doi:10.5194/gmd-9-2809-2016.
- Alessandri, F. Catalano, M. De Felice: Different Signatures of Land-Albedo Feedback on the Observed Northern Hemisphere Warming, Under submission
- Catalano F., Alessandri A., and co-authors Process-based enhancement of climate predictions in EC-Earth due to improved soil-moisture albedo feedback. In preparation.
- Doescher R, and co-authors: EC-Earth in CMIP6. Under submission in Geosci. Model Dev.

Future plans

(Please let us know of any imminent plans regarding a continuation of this research activity, in particular if they are linked to another/new Special Project.)

The process-based modelling developments in EC-Earth obtained in this special project will feed the activities that will be performed in the new special project SPITALES [2019-2021].